

MTMW20 Portfolio 2

The Hadley Cell and ENSO

March 2023

1 Introduction

The weather and climate are shaped by interconnected phenomena known as teleconnections, operating across various time scales, particularly from interannual to interdecadal scales. These interactions occur between the atmosphere and ocean, impacting environmental and socio-economic systems. Analysing these systems both in isolation and in conjunction, is crucial to understand how they interact to amplify and mitigate each other's effects. For instance, during El Niño events, the Hadley circulation strengthens, disrupting global rainfall patterns, leading to floods, human disease migration, and loss of life (Boers et al., 2019; Smith et al., 2015).

Understanding these phenomena, especially in the context of global warming, is crucial for effective mitigation and adaptation planning, notably in agriculture, policy making, and disaster management. Agriculture is particularly vulnerable to the impacts of climate change, as shifts in temperature and precipitation patterns can significantly affect crop yields and pest and disease dynamics. In a more novel example, Coburn (2021) finds that the enhanced predictability of seasonal wind forecasts, aiding in the strategic planning of wind farm projects and for the anticipation of periods of reduced power output. This would not only enhance the efficiency and reliability of renewable energy systems, as well as reducing our carbon footprint.

To explore such teleconnections, the Hadley cell is examined - an atmospheric circulation that transports warm, moist air poleward into the upper troposphere, and cool, dry air equatorward into the lower troposphere. At the ascending branch of the Hadley cell lies the Intertropical Convergence Zone (ITCZ) which characterised by intense convection and rainfall.

Various frameworks for predicting the width of the ITCZ independently from ENSO are discussed. One such model, the Held-Hou model, serves as a case study to qualitatively assess the circulation's relation and sensitivity to various parameters. Drawing from these findings and the previously discussed frameworks, the potential impacts of global warming on the Hadley circulation are postulated. The influence of the El Niño-Southern Oscillation (ENSO) on the ITCZ is subsequently examined, based the findings of Bain et al. (2011).

2 Theoretical Frameworks

Current understanding of the meridional extent of the Hadley cell is shaped by several non-mutually exclusive theoretical frameworks. The classic theory, developed pioneered by Held and Hou (1980), characterises the extent of the cell as:

$$\Phi \sim \left(\frac{gH_t\Delta_h}{\Omega^2 a^2 \theta_0} \right)^{\frac{1}{2}} \quad (1)$$

with g , the gravitational acceleration, H_t , the height of the tropical tropopause, Δ_h , the meridional potential temperature gradient (in radiative equilibrium), Ω , the rotation rate of Earth, a , the radius of Earth, and θ_0 , the global mean reference temperature Xian et al., 2021.

This model operates under the assumption that the upper tropospheric wind conserves angular momentum and is energetically closed with no net exchange of mass or thermal energy outside of

the cell. Baroclinic instabilities are suppressed, and the regions poleward of the Hadley cell are in radiative equilibrium.

An alternative framework, known as Phillips' criterion for baroclinic instability Phillips, 1954, scales the extent of the Hadley cell with a dependence on static stability:

$$\Phi \propto \left(\frac{NH_e}{\Omega a} \right)^{\frac{1}{2}} \quad (2)$$

with N , the vertical mean Brunt-Vaisala frequency which is proportional to the gross static stability of the troposphere, and H_e , the subtropical tropopause height Xian et al., 2021.

This criterion identifies the conditions for baroclinic instability that can lead to the development of cyclones and weather systems. According to this model, the extent of the cell coincides with the latitude at which the angular-momentum conserving Hadley circulation is terminated by linear baroclinic instability.

While the Held-Hou model suggests that the cell extent is proportional to the meridional temperature gradients and the tropical tropopause height, Phillip's criterion suggests it is proportional to the gross static stability and the local subtropical tropopause height. Based on simulation of atmospheric and coupled models, the latter scaling appears to provide a more accurate depiction of the dynamics of the Hadley cell within the present-day climate Xian et al., 2021.

Further insights into the role of baroclinic instability in the atmosphere can be gained through the Eady mode, proposed by Eady (1949). This model assumes a constant density (Boussinesq approximation) and neglects the effects of sphericity ($\beta = 0$), and predicts the maximum growth rate of baroclinic instabilities as:

$$\sigma_E \sim 0.31 \frac{f}{N} \frac{\partial u}{\partial z} = 0.31 \frac{f}{N} \frac{\Delta U}{H_e} \quad (3)$$

with f , the Coriolis parameter, $\partial U / \partial z$, the vertical wind shear, and ΔU , the difference in zonal wind between the upper and lower troposphere (Xian et al., 2021).

For an increased dry static stability in the subtropics, Lu et al. (2007) note that in order to maintain a constant baroclinic growth rate, the transient eddies must increase their 'f' value by moving poleward. Thus, such an increase in N , results in a greater Hadley cell extent.

These frameworks are collectively analysed in Section 4 and 5 to discern the influence of global warming and El Niño on the Hadley circulation.

2.1 Case Study: Held-Hou Model

A case study is conducted using a simple Held-Hou model in Python, developed by Charlton-Perez (2008), which aligns with the theory presented in §2 of the class notes. By inputting values for the parameters listed in Eq. 2, the model generates outputs for the zonally-averaged angular momentum conserving potential temperature, denoted as θ_m , and the equilibrium potential temperature with and without the inclusion of moisture in the model, represented as θ_e and θ_e^* , respectively. Fig. 1 presents a profile illustrative of this data.

The input variables are adjusted, and the resulting outputs are examined in terms of the strength and extent of the Hadley cell. Notably, the width of the moist heating zone, corresponds to the ITCZ, and is input as a fraction of the width of the heating zone in the dry case. Therefore, a moist heating scaling of 1 indicates that the ITCZ region represents the total cell width.

According to §2.3.1 of the class notes, the magnitude of the difference between the momentum conserving and equilibrium potential temperature is proportional to the strength of the meridional overturning. This difference is computed after vertically adjusting both curves to lie above the x-axis, and is computed for varying ITCZ width scalings (0 – 1), tropopause heights (8 – 12km), and meridional temperature gradients (30 – 60K), as shown in Fig. 2.

In the moist case in all plots, there is a non-linear but mostly inverse relation between the Hadley cell strength and the ITCZ width, tropical tropopause height, and meridional temperature gradient. In all plots, the overturning strength is greater than in the dry case.

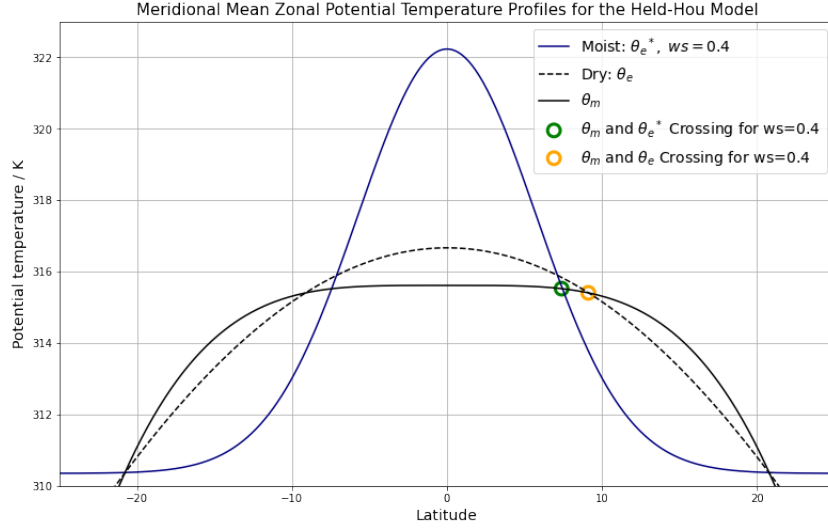


Figure 1: The equatorially-heated Held-Hou model solution is depicted by the mean zonal potential temperature profile, using a cell width scaling of 0.4. Solid blue and dashed black lines represent the equilibrium potential temperature for the moist and dry cases, respectively. The momentum conserving potential temperature is depicted in solid black for both scenarios. The closest equatorial intersection between momentum-conserving and equilibrium potential temperatures are indicated by yellow and green circles for the dry and moist cases, respectively.

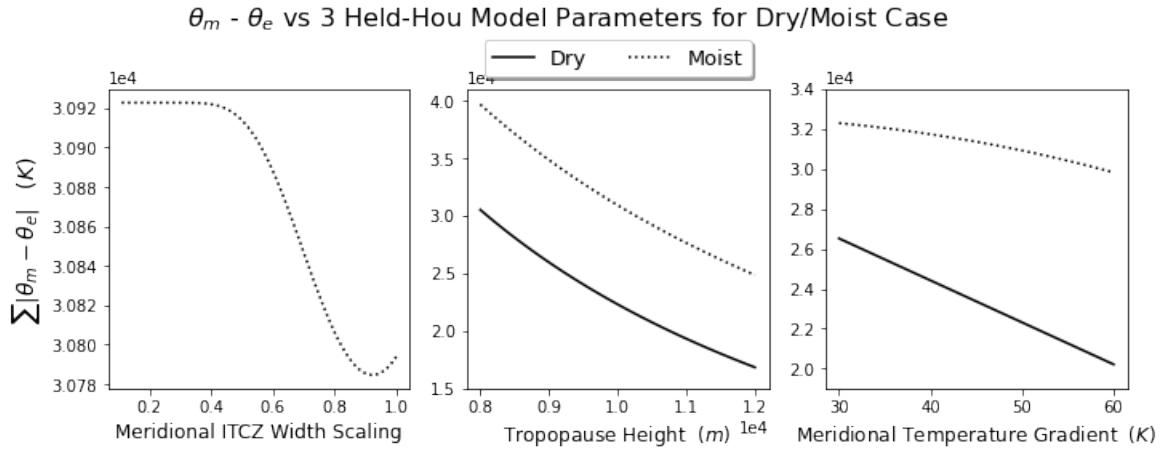


Figure 2: The vertically adjusted difference between momentum conserving and equilibrium potential temperatures, plotted against varying parameters for the dry and moist cases: meridional width scaling (left), tropical tropopause height (centre), and meridional temperature gradient (right). The strength of the meridional overturning is proportional to this potential temperature difference. The dry case for the ITCZ width scaling (not shown) is a horizontal line, as there is no ITCZ in the dry case.

By crudely examining the change in y-axis values ($\sum |\Delta\theta|$) for each plot, it is evident that the overturning strength is more sensitive to a 1K change in meridional temperature gradient (y-axis change of 82.5) than it is to a 1m change in the tropopause height (3.7), and is the least sensitive to a 0.1 change in width scaling between 0.1 and 0.4 width (2.7). However, it is crucial to interpret these sensitivities within the context of realistic shifts in these variables.

Fig. 2 depicts the change in both meridional and vertical velocities with the ITCZ extent. The meridional velocity is generally magnitudes greater than the vertical velocity and beyond a width scaling of ~ 0.3 , the meridional velocities approach 0, indicating that such a regime does not support an overturning ITCZ.

Furthermore, the latitude of the closest equatorial intersection between the momentum conserving and equilibrium potential temperature is depicted for the dry and moist case in Fig. 1, with an orange and green marker, respectively. According to §2.3.1 of the class notes, the former being smaller than the latter, is indicative of a decreased (increased) ascent (descent) width. Fig. 3 (right) depicts the change in this intersection with the ITCZ width scaling, and confirms that the moist model exhibits a decreased (increased) ascent (descent) width relative to the dry model.

Within the regime of a realistic width scaling (< 0.3), it becomes evident that the width of the ascent (descent) region expands (shrinks) as the ITCZ expands. However, beyond this scaling, it appears that the width of the ascent region does not continue to expand in-conjunction with the ITCZ. This discrepancy reveals a flaw in the analysis, suggesting that the equatorial distance of the intersection points does not reflect the degree of change in ascent/descent regions as anticipated.

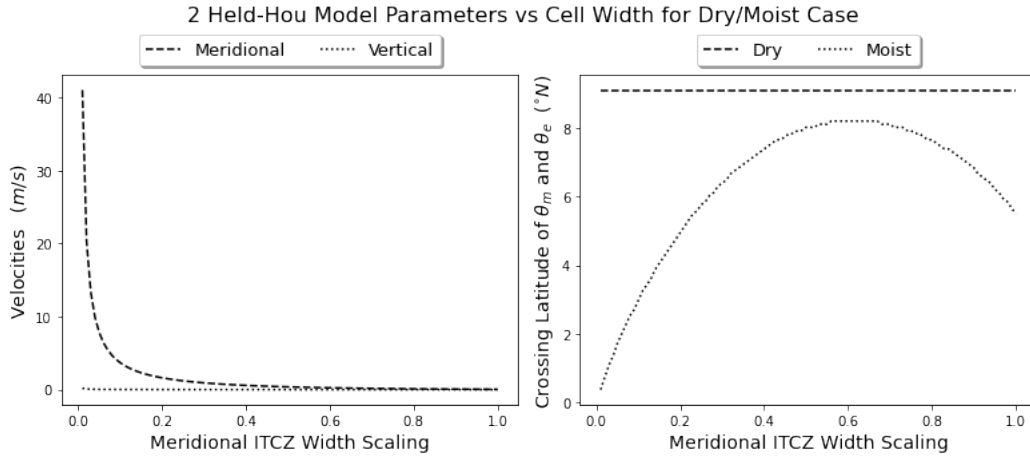


Figure 3: The meridional and vertical velocities (left), and the latitude of the closest equatorial intersection between momentum conserving and equilibrium potential temperatures (right) are plotted against the cell width scaling for both dry and moist cases.

Through experimentation with the model, it became apparent that the Held-Hou model is limited by its simple dynamics. Notably, in the moist model, the fractional change (scaling) of the moist and dry heating regions remains constant. However, research by Byrne and Schneider, 2016a using CMIP5 models demonstrates that these fractional changes are anticorrelated. Thus, for a given ITCZ expansion, the dry region contracts to a lesser degree, resulting in an overall expansion of the Hadley cell.

Overall, the case study finds that a potential 'worst-case scenario', characterised by a significant weakening of the Hadley circulation, may arise from a combination of a high tropopause, a steep meridional temperature gradient, and a large ITCZ width. The Held-Hou framework predicts that this scenario would manifest as an expanded Hadley cell, but fails to predict the likely occurrence of a contracted dry region.

3 Global Warming and the Hadley Circulation

Global warming, driven by increased greenhouse gas emissions, sees an increased absorption of long wavelength radiation and thus a warming of the atmosphere. In turn, vapour pressure increases in accordance with the Clausius Clapeyron equation, and the atmosphere’s capacity to hold water vapour increases.

According to the frameworks outlined in Section 1, various physical processes exert opposing influences on the width and strength of the Hadley cell including:

- An increased global mean temperature θ_0 , which results in an expansion of the Hadley cell according to the Held-Hou model. As discussed in the case study, this also coincides with a weakening of the overturning.
- A reduced meridional temperature gradient, stemming from increased surface-level warming at high latitudes, resulting in a contracted/strengthened Hadley cell.
- An increased static stability in the tropics due to surface and upper troposphere warming from greenhouse gases, and lower stratospheric cooling due to ozone depletion. This heightened stability provides more moisture for transient eddies to redistribute across the ITCZ and polewards. In fact, Byrne and Schneider (2016a) reports that the divergence of moist static energy by transient-eddies increases monotonically with warming in the ITCZ. This divergence is known to widen and weaken the Hadley cell, and is in accordance with the inverse relation of the cell extent and static stability in both Phillips’s and Eady’s frameworks.
- An elevated tropical and subtropical tropopause, attributable to higher surface temperatures and static stability. According to Held-Hou and Phillips this would result in the expansion of the Hadley cell. According to the Eady model, a higher subtropical tropopause also increases the critical shear necessary for the onset of baroclinic instability, thus leading to a poleward shift in the edge of the cell (Lu et al., 2007).
- Increased glacial melt, which redistributes ice mass from polar regions to oceans, effectively reducing the Earth’s moment of inertia and thus its rotation rate (Anderson, 2022). According to Held-Hou and Phillip, this would manifest as an expansion/weakening of the Hadley cell. The magnitude of this effect is likely to be smaller than other factors that influence the Earth’s rotation, such as prevailing winds.

Although these process have been presented individually, they interact with each other in a complex manner. In particular, the decreased meridional temperature gradient opposes the increased static stability, tropopause height and moist static energy divergence. While the relative significance of each process still remains debated within the literature, there is a general consensus of a widening and weakening Hadley circulation (Xian et al., 2021; Hu et al., 2018; Lu et al., 2007).

These findings point to the necessity of a comprehensive framework capable of integrating all of these processes. Byrne and Schneider (2016b) proposed a framework that explicitly accounts for changes in the net energy input into the atmosphere, the gross moist stability, the divergence of moist static energy by transient eddies, and the advection of moist static energy by the Hadley circulation. Unlike the Held-Hou model, it also incorporates the fractional changes between the ITCZ and descent regions.

4 ITCZ-ENSO Teleconnection

Fig. 4 of Bain et al. (2011) depicts a strong correlation ($r=0.67$) between the mean area of the ITCZ, determined from May-October IR-labels, and the multivariate ENSO index over the 1980-2010 period. High positive indices denote warm El Niño conditions, whereas large negative values signify La Niña conditions. Generally, warm phases coincide with an expanded ITCZ area, while cold phases exhibit the opposite trend. The magnitude of the warm/cold phase correlates to the

magnitude of the extent of the ITCZ, with warm phases being notably more intense, with comparable frequency to cold phases.

The ENSO-independent ITCZ signal reflects a combination of anthropogenic, naturally forced, and internally generated variability over interannual and interdecadal time scales. This separation of phenomena enables the identification of climate trends that might not be immediately discernible otherwise.

Phases with below-normal ITCZ area have comparable intensity to phases with above-normal area but tend to persist longer and occur more frequently. Overlaying the ENSO-independent signal with the dependent signal reveals the coherence and collocation of their minima and maxima, albeit with some discrepancies in magnitude. These findings suggest that ENSO may modulate the intensity and frequency of ITCZ phases. Despite the removal of ENSO influence, the strong coherence between these signals may be partially attributed to the independent signal being derived only from years when the ENSO index exceeds $|0.5|$, resulting in a reduced but not completely eliminated influence. This coherence may also imply a complex and potentially nonlinear or lagged relationship between the ITCZ and ENSO, or the presence of an unaccounted common climate mode.

Additionally, the absence of any discernible trend in the independent signal may stem from the relatively short 30-year time series duration.

Considering the increased tropical tropopause height during El Niño, these findings seem to be consistent with the meridional expansion predicted by the Held-Hou model. However, much of the most recent scientific literature indicates a narrowing and strengthening of both the Hadley cell and ITCZ during El Niño, and conversely during La Niña (Lu et al., 2007; Hu et al., 2018; Fan et al., 2018). This raises questions about the direct correlation between the ITCZ area computed by Bain et al. (2011) and the meridional ITCZ width computed by the aforementioned studies. Additionally, it questions whether the Held-Hou model can differentiate between a localised warming anomaly such as El Niño and a global warming anomaly resulting from climate change.

Moreover, it is widely anticipated that global warming, despite not apparent in Bain et al. (2011), will likely lead to an increase in both the frequency of intense El Niño events (Tang et al., 2016). The interaction between the narrowing effects of El Niño, and the widening effects of global warming introduces another level of complexity to understanding the future of the Hadley circulation.

5 Conclusion

Given the profound socioeconomic and environmental impacts of teleconnections, improved predictability of such systems is imperative, particularly amid the uncertainties posed by global warming. This necessitates a comprehensive understanding of systems such as the Hadley circulation and ENSO, both in isolation and in tandem.

Analysing a simple Held-Hou model has revealed key dynamics of the Hadley circulation, indicating how its strength varies as the ITCZ expands and how moisture affects the width of the ascent and descent regions. Although the model's simplicity limits its representation of more complex circulation dynamics, it provides some valuable qualitative insights.

In terms of its teleconnection, the Hadley cell is examined with and without the influence of ENSO. However, the relevance of the findings within the context of the Held-Hou model and other literature is unresolved.

These findings, combined with the frameworks of Phillips and Eady, enable the impacts of global warming on the Hadley circulation to be reasoned. It is shown that variability in the Hadley cell is the result of a delicate balance between many competing effects.

A comprehensive understanding of the the Hadley circulation, and thus its teleconnection with ENSO, may necessitate one unified framework, an urgent challenge posed by the immediacy of climate change.

References

- Boers, N., Goswami, B., Rheinwalt, A., Bookhagen, B., Hoskins, B., & Kurths, J. (2019). Complex networks reveal global pattern of extreme-rainfall teleconnections. *Nature*, *566*, 373. <https://doi.org/10.1038/s41586-018-0872-x>
- Smith, K. R., Woodward, A., Campbell-Lendrum, D., Chadee, D. D., Honda, Y., Liu, Q., Olwoch, J. M., Revich, B., Sauerborn, R., Confalonieri, U., Haines, A., Chafe, Z., & Rocklov, J. (2015). Human health: Impacts, adaptation, and co-benefits. <https://doi.org/10.1017/CBO9781107415379.016>
- Coburn, J. (2021). Climatological teleconnections with wind energy in a midcontinental region. *Journal of Applied Meteorology and Climatology*, *60*, 305–322. <https://doi.org/10.1175/JAMC-D-20-0203.1>
- Bain, C. L., Paz, J. D., Kramer, J., Magnusdottir, G., Smyth, P., Stern, H., & Wang, C. C. (2011). Detecting the itcz in instantaneous satellite data using spatiotemporal statistical modeling: Itcz climatology in the east pacific. *Journal of Climate*, *24*, 216–229. <https://doi.org/10.1175/2010JCLI3716.1>
- Held, I. M., & Hou, A. Y. (1980). Nonlinear axially symmetric circulations in a nearly inviscid atmosphere. *Journal of the Atmospheric Sciences*, *37*, 515–533. [https://doi.org/10.1175/1520-0469\(1980\)037<0515:NASCIA>2.0.CO;2](https://doi.org/10.1175/1520-0469(1980)037<0515:NASCIA>2.0.CO;2)
- Xian, T., Xia, J., Wei, W., Zhang, Z., Wang, R., Wang, L. P., & Ma, Y. F. (2021). Is hadley cell expanding? <https://doi.org/10.3390/atmos12121699>
- Phillips, N. A. (1954). Energy transformations and meridional circulations associated with simple baroclinic waves in a two-level, quasi-geostrophic model. *Tellus A: Dynamic Meteorology and Oceanography*, *6*, 273–286. <https://doi.org/10.3402/tellusa.v6i3.8734>
- Lu, J., Vecchi, G. A., & Reichler, T. (2007). Expansion of the hadley cell under global warming. *Geophysical Research Letters*, *34*, 1–4. <https://doi.org/10.1029/2006GL028443>
- Byrne, M. P., & Schneider, T. (2016a). Narrowing of the itcz in a warming climate: Physical mechanisms. *Geophysical Research Letters*, *43*, 1135. <https://doi.org/10.1002/2016GL070396>
- Anderson, L. W. (2022). Changes in the earth’s rotation rate due to global warming. *Journal of Earth Science and Climatic Change*, *13*, 1–3.
- Hu, Y., Huang, H., & Zhou, C. (2018). Widening and weakening of the hadley circulation under global warming. <https://doi.org/10.1016/j.scib.2018.04.020>
- Byrne, M. P., & Schneider, T. (2016b). Energetic constraints on the width of the intertropical convergence zone. *Journal of Climate*, *29*, 4716–4717. <https://doi.org/10.1175/JCLI-D-15-0767.1>
- Fan, J., Meng, J., Ashkenazy, Y., Havlin, S., & Schellnhuber, H. J. (2018). Climate network percolation reveals the expansion and weakening of the tropical component under global warming. *Proceedings of the National Academy of Sciences of the United States of America*, *115*, 12128–12134. <https://doi.org/10.1073/pnas.1811068115>
- Tang, T., Li, W., & Sun, G. (2016). Impact of two different types of el ninõ events on runoff over the conterminous united states. *Hydrology and Earth System Sciences*, *20*, 28–37. <https://doi.org/10.5194/hess-20-27-2016>